

# Contact network models matching the dynamics of the COVID-19 spreading

Matúš Medo<sup>1,2,3</sup>

<sup>1</sup>*Department of Radiation Oncology, Inselspital, University Hospital of Bern,  
and University of Bern, 3010 Bern, Switzerland*

<sup>2</sup>*Institute of Fundamental and Frontier Sciences,  
University of Electronic Science and Technology of China, Chengdu 610054, PR China*

<sup>3</sup>*Department of Physics, University of Fribourg, 1700 Fribourg, Switzerland\**

We study the epidemic spreading on spatial networks where the probability that two nodes are connected decays with their distance as a power law. As the exponent of the distance dependence grows, the model networks smoothly transition from the random network limit to the regular lattice limit. We show that despite keeping the average number of contacts constant, the increasing exponent hampers the epidemic spreading by making long-distance connections less frequent. The spreading dynamics is also influenced by the exponent value and changes from exponential growth to power-law growth. The observed power-law growth is compatible with recent analyses of the COVID-19 spreading in numerous countries.

## I. INTRODUCTION

Mathematical modeling of epidemic processes has a long tradition [1–3]. After the rise of the network science [4, 5], the study of epidemics spreading on networks has inevitably led to a flourishing of literature [6–9]. This has led to novel insights including the impact of network hubs [10], long-distance connections [11], and the effective spreading geometry [12] on the epidemic spreading.

By contrast, efforts addressing epidemics on spatial networks with prevailing short connections are comparatively few. In view of the unprecedented movement and activity restrictions that are being introduced in countries across the globe to curb the spreading of the new virus COVID-19 [13], this is a research gap that calls to be addressed. Of particular interest are the temporal patterns of the COVID-19 epidemic as there is now extensive empirical evidence that the progress of COVID-19 is power-law in China [14–16], Chinese provinces [17, 18], as well as other countries [18, 19]. Power law growth is very different from the classical exponential growth that follows from the assumption of homogeneous mixing [1, 2]. In [17], the authors propose a modified SIR model which assumes that the supply of susceptible individuals gradually decreases as a consequence of the implemented containment policies. While the model produces sub-exponential growth and fits the data (prior to February 12) well, the connection between containment policies which are typically introduced abruptly (such as a curfew issued by a government) and gradual depletion of susceptible individuals is unclear. On scale free networks with a diverging second moment of the degree distribution, early power law growth with the exponent  $D - 1$  where  $D$  is the network diameter (the maximal distance between two nodes in the graph) has been found for the SI epidemic model [20].

We study here epidemic spreading on model spatial

networks introduced in [21] where a single parameter can be used to gradually shift from a random network limit where the spatial node distance is of little importance and long-range connections are common to a regular lattice limit where only the nearest-neighbors are connected. In close similarity with the classical Watts-Strogatz model [22], small-world networks (networks with high clustering and small average distance between the nodes) are produced for intermediate values of this network parameter. Epidemic spreading in the lattice limit is well understood and characteristic by quadratic growth [23]. The spatial network model thus allows us to study the continuous transition between quadratic and exponential growth. A comparison with empirical growth curves in turn gives us insights into the contact network that supports the spreading. While contact tracking yields the best source of information on the contact network, the contact tracking data is not available now. Investigating the effect of various contact network topologies on the epidemic spreading is hence the only viable option of gaining insights in the contact network structure.

We find that spatial networks where short links are favored support epidemic spreading significantly less than random networks. The spatial network structure, together with epidemic characteristics of a considered pathogen, is thus crucial for the final extent of an outbreak. Furthermore, the epidemic dynamics in these network features power-law growth with exponents varying in a broad range depending on the network characteristics, in agreement with extensive empirical evidence of power-law growth for the COVID-19 pandemic [14–19]. Our results thus provide an indirect way of probing the structure of actual contact networks over which the virus spreads, as well as suggestions for making these networks less permissible to the virus. Note that we purposely avoid the question of epidemic predictions which has been addressed using phenomenological fits [24–26] and extensive agent-based models [27] elsewhere.

---

\* [matus.medo@unifr.ch](mailto:matus.medo@unifr.ch)

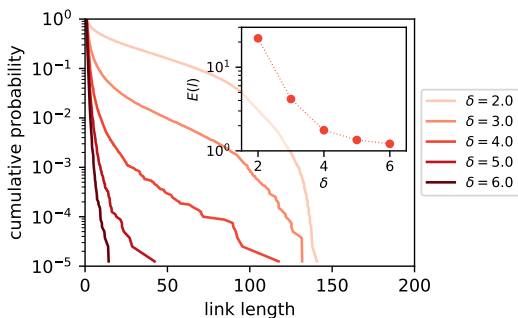


FIG. 1. The distribution of link lengths in model spatial networks with  $N = 40,000$ . For each  $\delta$ ,  $\lambda$  is chosen to achieve the chosen mean degree  $z = 4$ . Note that for this  $N$ , the longest possible link is  $\sqrt{N}/\sqrt{2} \approx 141$ . The inset shows the mean link length,  $E(l)$ , as a function of the exponent  $\delta$ .

## II. A SPATIAL NETWORK MODEL

In a spatial complex network, the probability that two nodes are connected is given by the distance between them [7]. We use here the model introduced in [21] where  $N$  nodes form a two-dimensional square lattice with periodic boundary conditions; we assume for simplicity that  $N = S^2$  where  $S$  is a natural number. In this model, the probability that two nodes are connected depends only on their distance  $d$ , hence the label “network with distance-dependent connectivity”, as

$$P(d) = \frac{1}{1 + \lambda d^\delta} \quad (1)$$

where  $\lambda$  and  $\delta$  are model parameters. By contrast to the simpler form  $P(d) \sim d^{-\delta}$  used in [28], the absolute term in the denominator conveniently avoids a divergence of  $P(d)$  when  $d \rightarrow 0$ . The exponent  $\delta$  determines how fast  $P(d)$  decays with distance and  $\lambda$  can be used to achieve a desired mean degree,  $z$ , in the resulting network. In [21], the authors show that  $2.5 \gtrsim \delta \lesssim 3.5$  produces small-world networks where the average shortest paths are “short” and the clustering coefficient values are high. The model thus formalizes what has been anticipated by previous analyses of the COVID-19 data: “individuals have many local neighbors and occasional long-range connections” [15].

Figure 1 shows that as  $\delta$  grows, links in model networks become shorter. In the limit  $\delta \rightarrow \infty$ , only the shortest links are possible and the network becomes regular: each node is connected with its  $z$  closest neighbors. The opposite limit,  $\delta \rightarrow 0$ , is also instructive: node distance then becomes irrelevant and the connection probability is the same,  $1/(1 + \lambda)$ , for all nodes. We thus recover a classical random network [29].

The original spatial model produces a narrow degree distribution which is typically not a good fit for real social networks [30, 31]. This limitation can be overcome by assigning specific  $\lambda$  values to all nodes and making

Eq. (1) dependent on the  $\lambda$  values of the considered pair of nodes [32]. We use

$$P(d_{ij}) = \frac{1}{1 + \min(\lambda_i, \lambda_j) d^\delta} \quad (2)$$

as the probability that nodes  $i$  and  $j$  with distance  $d_{ij}$  and respective values  $\lambda_i$  and  $\lambda_j$  are connected. Note that a smaller  $\lambda$  value in Eq. (1) leads to a higher connection probability. By using the minimum  $\lambda$  value in Eq. (2), we thus make it possible that a node with a small  $\lambda$  value connects with many nodes in the network. Albeit this choice slightly differs from the one used in [32], the tail behavior of the degree distribution remains unchanged. In particular,  $\lambda$  distributed among the nodes as  $\varrho(\lambda) \sim \lambda^x$  in  $\lambda \in (0, \lambda_{\max}]$  has been shown in [32] to lead to a power-law tail of the degree distribution with the exponent  $\gamma = \delta(x + 1)/2$ . The upper bound of the  $\lambda$  distribution,  $\lambda_{\max}$  directly determines the mean degree. We use this approach to generate spatial networks with the degree distribution exponents 3.5 and 2.5, respectively. We use the basic network model characterized by a single  $\lambda$  value and Eq. (1) unless stated otherwise.

## III. AN EPIDEMIC MODEL

We use an SEIR epidemic model [2, 33] where each node can be in one of four possible states: susceptible (S), exposed (E), infected (I), and recovered (R). While the choice of the model and its parameters are motivated by the ongoing COVID-19 epidemic (see [34, 35] for the latest epidemiology information on COVID-19), the presented findings do not change qualitatively when a different model or a different set of parameters are used.

All nodes are initially susceptible except for one node which is exposed. The exposed nodes represent the individuals who have already contracted the disease but have not developed the symptoms yet. In the case of COVID-19, these individuals have been shown to considerably contribute to spreading the disease [36]. The simulation runs in time steps with one step representing one day. If susceptible node  $i$  is connected with an exposed node, the probability that node  $i$  becomes exposed is  $\beta_1$ . If susceptible node  $i$  is connected with an infected node, the probability that node  $i$  becomes exposed is  $\beta_2$ .

While the infection process is probabilistic, we assume for simplicity that the disease progression is deterministic: If node becomes exposed at time  $t$ , it automatically becomes infected (develops disease symptoms) at time  $t + T_1$  and recovered at time  $t + T_1 + T_2$ . Here  $T_1$  is the incubation period and  $T_2$  is the recovery time. Recovered nodes cannot contract the disease again.

We use  $T_1 = 5$ ,  $T_2 = 14$ , and  $\beta_2/\beta_1 = 0.2$  (this reflects the role of asymptomatic agents in the spreading process [36]). We simulate 300 time steps of the epidemic spreading. We run 10,000 independent realizations of the epidemic process and use the median to find a representative epidemic outcome at any time point. We measure the

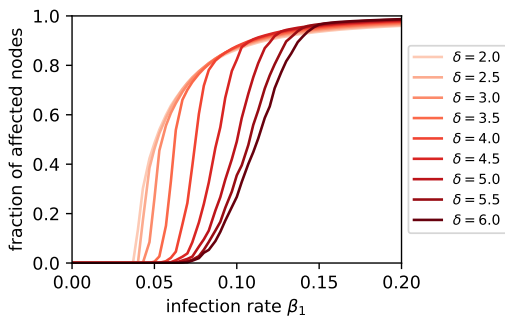


FIG. 2. The fraction of infected nodes at  $t = 300$  for  $N = 40,000$  and  $z = 4$  as a function of the infection rate.

epidemic spreading using the number of affected nodes which includes exposed, infected and recovered nodes, so it is naturally a cumulative metric which quantifies how many nodes have contracted the disease during the simulation time.

#### IV. EPIDEMIC DYNAMICS ON MODEL NETWORKS

We present here results of numerical simulations of epidemic spreading on model spatial networks. Before addressing the dynamics of the epidemic process, Figure 2 shows that the spatial distribution of links, controlled in the model by the exponent  $\delta$ , has strong influence on the epidemic spreading. In particular, the fraction of infected nodes at a given time decreases as  $\delta$  grows. This is a direct consequence of the spatially-constrained epidemic spreading when  $\delta$  is large: Many neighbors of an infected node are then already infected, so the node’s effective ability to spread the disease further is reduced. By contrast, neighbors of an infected node in a random network are unlikely to be already infected (unless a significant fraction of all nodes have been infected) which facilitates further spreading. In summary, the epidemic spreading can be effectively reduced by both lowering the number of contacts (in particular close contacts with whom we spend prolonged time indoors, for example) as well as by purposely choosing nearby contacts. A comparatively higher number of strongly localized social contacts can lead to the same final fraction of infected population as a lower number of widely distributed social contacts.

The effect of  $\delta$  can be readily understood by inspecting the spreading patterns for various values of  $\delta$  shown in Figure 3. When  $\delta$  is high ( $\delta = 6$ ), the epidemic spreads as on a regular lattice and develops a clearly-defined spreading front. Nodes on the front, that can spread the infection further, can only spread it in one direction (outwards) which limits their effective reproduction number (number of nodes that they infect on average). As  $\delta$  decreases, the spreading front first becomes “diffuse” ( $\delta = 4$ ) until it “dissolves” entirely ( $\delta = 2$ ). The

epidemic then spreads more effectively as it is more probable that a neighbor of an infected nodes is susceptible to the infection.

We now return to the main question: the effect of the spatial network structure on the dynamics of epidemic spreading. This dynamics has two well known special cases. On a random contact network, the assumption of homogeneous mixing of susceptible and infected nodes is valid and one recovers the exponential epidemic growth [2]. On a regular two dimensional lattice with nearest-neighbor connections, the epidemic spreading instead develops an epidemic front that propagates at a constant velocity. The front’s constant velocity then directly implies that the radius of the affected area grows linearly with time and, consequently, the number of infected individuals grows quadratically with time [23].

Spatial networks with distance-dependent connectivity give us the possibility to smoothly transition between the two extremes. We can thus directly observe how quadratic growth on a lattice changes in exponential growth on a random network. Figure 3 provides the first indication with the epidemic front becoming more diffuse and the speed of its propagation grows as  $\delta$  decreases. As this happens, the argument leading to quadratic growth ceases to be valid and we expect the growth to be faster than quadratic. This is confirmed by Figure 4 where we show the epidemic dynamics for various contact networks. Growth that is of a power-law kind (it follows a straight line over a substantial part of the log-log plane in panel A) for the 2D lattice as well as for the spatial networks with  $\delta \gtrsim 4$  becomes clearly exponential for the random network and for the spatial network with  $\delta = 2$  (see the straight lines in the log-linear panel B). Note that the results obtained on random networks and the regular square lattice are very close to the displayed results for  $\delta = 2$  and  $\delta = 6$ , respectively.

We find that quadratic epidemic growth on 2D lattices generalizes to power-law growth on the model spatial networks with sufficiently high exponent  $\delta$ . Table I shows that for the data shown in Figure 4A, stable estimates of the growth exponent (indicating good power-law fits of the data) can be obtained for  $\delta$  greater or equal to 4. The resulting power-law growth exponents supported by simulations with  $N = 160,000$  nodes lie in the range 2–3.25 (for  $\delta = 3$ , power law ceases to fit well). As  $N$  grows, the range of  $\delta$  where a power-law fits the data well seems to expand. Notably, the power-law exponent is more than two even for the square lattice (for the same fitting as in Table I, we obtain 2.17–2.19). This is due to the probabilistic nature of the spreading that results in non-vanishing randomness of the spreading front that can be well seen in the first panel of Figure 3.

In [37], an SIR model on spatial networks with distance-dependent connectivity has been studied in a one-dimensional geometry (instead of the plane as we consider here). Instead of power-law growth, the authors use a different (and more complicated) functional form to fit their simulation results. In [19, 38], the authors

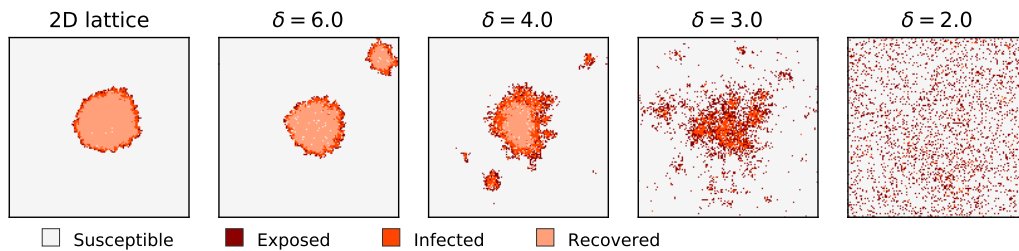


FIG. 3. Epidemic spreading on the square lattice and model spatial networks with various values of the exponent  $\delta$ . We use  $N = 160,000$  and  $z = 4$ . The snapshots are taken when 10% of all nodes had been affected by the epidemic. We use  $\beta_1 = 0.16$  for which half of all nodes become affected at the end of simulation for  $\delta = 6$ .

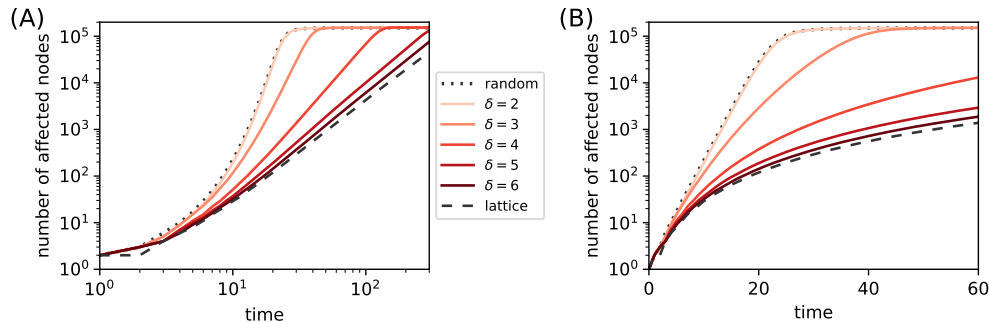


FIG. 4. Time evolution of the number of affected nodes for various contact networks. While the solid lines show results for spatial networks generated with different exponent values in Eq. (1), the dotted and dashed lines show results for a random network and a regular lattice, respectively. Straight lines in the log-log panel (A) are indicative of power-law growth. Straight lines in the log-linear panel (B) are indicative of exponential growth. As in Figure 3, we use  $N = 160,000$ ,  $z = 4$ , and  $\beta_1 = 0.160$ . We display here median over 10,000 epidemic realizations on a single network.

observe power-law growth in various countries and infer that the underlying networks must be scale-free and small-world (the small-world property is hypothesized also in [15, 16]). We see now that this is not necessarily the case. The model networks considered here can produce power-law growth when  $\delta \gtrsim 4$  yet they have narrow degree distributions [32] (*i.e.*, they are not scale-free) and [21] shows that high exponents in the distance dependence do not generate sufficiently many long-range links for the small-world phenomenon to emerge. We find that power-law growth with an exponent above two suggests that the contact network is spatially embedded and consists predominantly of short links; in the first order, it is a perturbation of a regular nearest-neighbor lattice.

We finally explore how variations of the underlying network change the estimated power-law growth exponents,  $\hat{b}$  (see Table I for the detailed results). When the mean degree increases,  $\hat{b}$  increases and this increase is more pronounced (up to 9%) for small  $\delta$  values. This is actually expected as higher  $z$  means that nodes on the epidemic front have more opportunities to have long-distance connections which in turn propel the front's movement forward. An increase of  $\hat{b}$  can be also observed when Eq. (2) is used to produce spatial networks with a power-law degree distribution. When the degree distribution expo-

TABLE I. Power-law exponents,  $\hat{b}$ , estimated by fitting straight lines to the data in Figure 4A. To focus on the straight part of the dependencies, we fit only the values below  $N/2$  infected cases and above 100–800 infected cases. The reported ranges of the fitted exponents are obtained by varying the fitting lower bounds. The exponent estimates for  $\delta = 3$  vary in comparatively broader ranges, indicating that power-law growth is not a good fit in this case (the same is true for  $\delta = 2$ , results not shown). The first two rows show results for the basic spatial network model with different mean degree values,  $z$ . The following two rows show results for the spatial network model with specified degree distribution exponents,  $\gamma$ .

	$\delta$	3	4	5	6
$\hat{b}(z = 4)$	5.25–5.60	3.23–3.26	2.42–2.44	2.29–2.31	
$\hat{b}(z = 10)$	5.52–5.86	3.53–3.56	2.51–2.56	2.33–2.38	
$\hat{b}(z = 4, \gamma = 3.5)$	5.67–5.87	3.65–3.67	2.67–2.69	2.44–2.45	

nent is  $\gamma = 3.5$ ,  $\hat{b}$  increases by up to 13% with respect to the original model with  $z = 4$ . Interestingly, power-law epidemic growth then appears to fit the data even better (*e.g.*, the exponent ranges in Table I are narrower) than for the original networks with narrow degree distributions. While the networks' fractal dimensions [28]

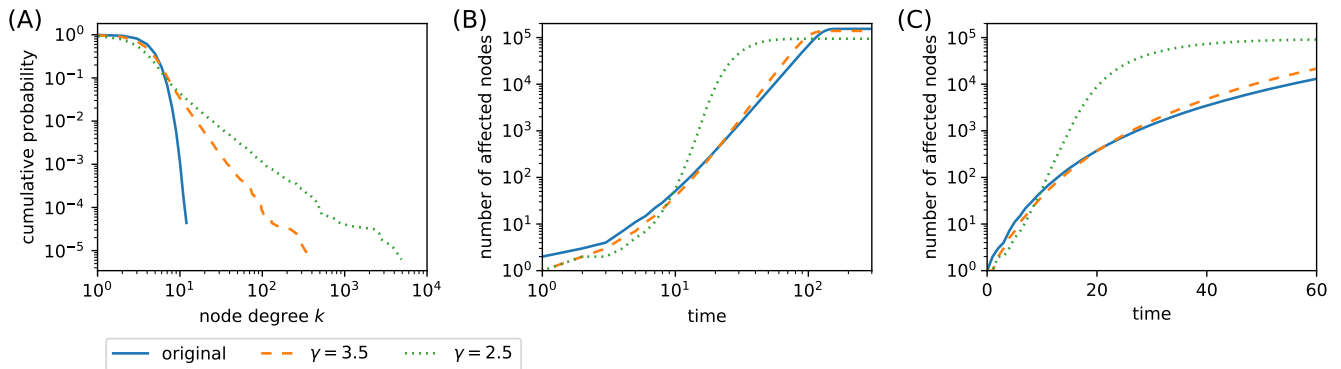


FIG. 5. Results for spatial networks with various degree distributions: original model with a narrow degree distribution and power-law distributions with exponents 3.5 and 2.5, respectively. We show here the representative results obtained with  $\delta = 5$ . Panel (A) shows the networks' degree distributions (for the two broad distributions, their fits based on likelihood maximization [39] yield exponents 3.50 and 2.51, respectively, when the fitting lower bound 20 is used, thus validating our network construction). Panels (B) and (C) show the epidemic dynamics in the log-log and log-linear layout, respectively. We use  $N = 160,000$  and  $z = 4$ . The transmission rates are  $\beta_1 = 0.160$  (original model),  $\beta_1 = 0.116$  ( $\gamma = 3.5$ ), and  $\beta_1 = 0.063$  ( $\gamma = 2.5$ ) for which, as we already used in Figure 3, half of all nodes become affected at the end of simulation for  $\delta = 6$ .

are similar to the power-law exponents obtained by fitting the epidemic growth, substantial differences (*e.g.*, around 0.4 for  $z = 10$  and  $\delta = 4$ ) can be observed in some cases. Differences between the fractal dimension and the epidemic growth exponents are expected to further magnify when link weights affecting the epidemic spreading are introduced.

The situation becomes very different when the degree distribution exponent  $\gamma$  is 2.5: the power-law parts of the epidemic growth then have substantially higher exponents (4.2 for  $\delta = 6$  and 5.9 for  $\delta = 5$ ). However, the range over which power-law growth can be observed shrinks substantially and exponential growth is a satisfactory description of the growth pattern. This is illustrated in Figure 5 which shows a direct comparison of the growth dynamics on original spatial networks and spatial networks with power-law degree distributions. Results remain qualitatively the same when a different infection rate  $\beta_1$  is used. The change of behavior for  $\gamma = 2.5$  is a direct consequence of a diverging second moment of the degree distribution,  $\langle k^2 \rangle$ , for a power-law exponent below 3;  $\langle k^2 \rangle$  has been shown crucial for the epidemic spreading on networks with heterogeneous degree distributions [10].

## V. DISCUSSION

In this work, we studied the interplay between the functional form of the connection probability in spatial networks and the dynamics of epidemic spreading on them. There are two main findings. Firstly, short (localized) links hinder the spreading. A better outcome (fewer infections and slower growth) can be thus achieved by limiting distant contacts even if the mean number of contacts remains fixed. Secondly, when short links are frequent in the network, the number of infected individuals

grows as a power-law instead of the canonical exponential epidemic growth. In the framework of the chosen connection probability decaying with node distance as a power law, frequent short links are achieved when the exponent of the connection probability decay is sufficiently high. In our simulations in particular, power law growth of the number of infections emerges when this decay exponent is greater than three. This observation is particularly relevant as the latest data show that the COVID-19 spreading in most countries indeed follows a power-law pattern instead of exponential growth. In other words, our results suggest that the social contacts over which the virus spreads are now extraordinary short which helps us to avoid the exponential spreading and thus give us more time for necessary actions.

We stress that the studied mechanism leading to power law growth of the number of infections is very different from the setting studied in [20] where a diverging second moment of the degree distribution is the main reason for sub-exponential growth. It remains open whether the degree distribution of the effective contact network has a diverging second moment during a major epidemic outbreak which necessarily affects the behavior of individuals and incites significant government interventions and society-wide restrictions. By contrast, the original spatial model that we consider here produces narrow (Poissonian) degree distributions, yet we find power-law epidemic growth as a consequence of spatially-constrained linking patterns which in turn determine the spreading dynamics. The result obtained in [20] in fact includes power law growth combined with exponential decay. While this exponential decay term can be conveniently used to fit the slowing epidemic data [26], the original source of this decay is the shrinking size of the susceptible population which, fortunately, is not a significant effect for COVID-19 which has yet affected a minor

fraction of the population. In the scope of fitting the COVID-19 data, the exponential term has to be thus viewed as phenomenological.

To better understand the impact of various features of the contact network on the resulting epidemic spreading, several modifications and generalizations of the network model can be studied in the future: (1) replacing individual nodes with households where each node has local connections to all other household members and

distance-dependent connectivity is only used to model the connections across the households and (2) introducing link weights that represent the intensity of the social contact and naturally play a role in the disease transmission. Finding an analytical relation between the connectivity decay exponent  $\delta$  and the epidemic growth exponent and formulating effective differential equations that describe the epidemics dynamics on spatial networks are other important directions.

- 
- [1] W. O. Kermack and A. G. McKendrick, Proceedings of the Royal Society of London, Series A **115**, 700 (1927).
- [2] O. Diekmann and J. A. P. Heesterbeek, *Mathematical epidemiology of infectious diseases: Model building, analysis and interpretation*, Vol. 5 (John Wiley & Sons, 2000).
- [3] F. Brauer, Infectious Disease Modelling **2**, 113 (2017).
- [4] A.-L. Barabási *et al.*, *Network science* (Cambridge University Press, 2016).
- [5] M. Newman, *Networks* (Oxford University Press, 2018).
- [6] M. J. Keeling and K. T. Eames, Journal of the Royal Society Interface **2**, 295 (2005).
- [7] M. Barthélemy, Physics Reports **499**, 1 (2011).
- [8] R. Pastor-Satorras, C. Castellano, P. Van Mieghem, and A. Vespignani, Reviews of Modern Physics **87**, 925 (2015).
- [9] M. A. Porter and J. P. Gleeson, Frontiers in Applied Dynamical Systems: Reviews and Tutorials **4** (2016).
- [10] R. Pastor-Satorras and A. Vespignani, Physical Review E **63**, 066117 (2001).
- [11] D. Balcan, V. Colizza, B. Gonçalves, H. Hu, J. J. Ramasco, and A. Vespignani, Proceedings of the National Academy of Sciences **106**, 21484 (2009).
- [12] D. Brockmann and D. Helbing, Science **342**, 1337 (2013).
- [13] W. H. Organization *et al.*, (2020).
- [14] A. Brandenburg, arXiv preprint arXiv:2002.03638 (2020).
- [15] A. L. Ziff and R. M. Ziff, medRxiv preprint 2020.02.16.20023820 (2020).
- [16] M. Li, J. Chen, and Y. Deng, arXiv preprint arXiv:2002.09199 (2020).
- [17] B. F. Maier and D. Brockmann, arXiv preprint arXiv:2002.07572 (2020).
- [18] B. Gross, Z. Zheng, S. Liu, X. Chen, A. Sela, J. Li, D. Li, and S. Havlin, arXiv preprint arXiv:2003.08382 (2020).
- [19] C. Manchain, E. L. Brugnago, R. M. da Silva, C. F. O. Mendes, and M. W. Beims, arXiv preprint arXiv:2004.00044 (2020).
- [20] A. Vazquez, Physical Review Letters **96**, 038702 (2006).
- [21] M. Medo, Physica A: Statistical Mechanics and its Applications **360**, 617 (2006).
- [22] D. J. Watts and S. H. Strogatz, Nature **393**, 440 (1998).
- [23] S. Riley, K. Eames, V. Isham, D. Mollison, and P. Trapman, Epidemics **10**, 68 (2015).
- [24] L. Jia, K. Li, Y. Jiang, X. Guo, *et al.*, arXiv preprint arXiv:2003.05447 (2020).
- [25] K. Wu, D. Darcet, Q. Wang, and D. Sornette, arXiv preprint arXiv:2003.05681 (2020).
- [26] R. Kollar and K. Bodova, Unpublished.
- [27] S. L. Chang, N. Harding, C. Zachreson, O. M. Cliff, and M. Prokopenko, arXiv preprint arXiv:2003.10218 (2020).
- [28] L. Daqing, K. Kosmidis, A. Bunde, and S. Havlin, Nature Physics **7**, 481 (2011).
- [29] B. Bollobás and B. Béla, *Random graphs* (Cambridge University Press, 2001).
- [30] Y.-Y. Ahn, S. Han, H. Kwak, S. Moon, and H. Jeong, in *Proceedings of the 16th International Conference on World Wide Web* (2007) pp. 835–844.
- [31] S. P. Borgatti, M. G. Everett, and J. C. Johnson, *Analyzing social networks* (Sage, 2018).
- [32] M. Medo and J. Smrek, The European Physical Journal B **63**, 273 (2008).
- [33] H. W. Hethcote, SIAM Review **42**, 599 (2000).
- [34] Q. Li, X. Guan, P. Wu, X. Wang, L. Zhou, Y. Tong, R. Ren, K. S. Leung, E. H. Lau, J. Y. Wong, *et al.*, New England Journal of Medicine (2020).
- [35] Y. M. Bar-On, A. I. Flamholz, R. Phillips, and R. Milo, arXiv preprint arXiv:2003.12886 (2020).
- [36] R. Li, S. Pei, B. Chen, Y. Song, T. Zhang, W. Yang, and J. Shaman, Science (2020).
- [37] A. Khaleque and P. Sen, Journal of Physics A: Mathematical and Theoretical **46**, 095007 (2013).
- [38] H. Singer, arXiv preprint arXiv:2003.11997 (2020).
- [39] A. Clauset, C. R. Shalizi, and M. E. Newman, SIAM Review **51**, 661 (2009).